arXiv:1704.01659v1 [cond-mat.stat-mech] 5 Apr 2017

Trapping Probability and Superdiffusive Motion on a Disordered Ratchet Potential

D.G. Zarlenga,[1] G.L. Frontini,[2] F. Family,[3] and C.M. Arizmendi[1]

[1]*Instituto de Investigaciones Científicas y Tecnológicas en Electrónica (ICYTE), Facultad de Ingeniería, Universidad Nacional de Mar del Plata, Av. J.B. Justo 4302, 7600 Mar del Plata, Argentina*

[2]*Instituto de Investigaciones en Ciencia y Tecnología de Materiales (INTEMA), Facultad de Ingeniería, Universidad Nacional de Mar del Plata, Av. J.B. Justo 4302, 7600 Mar del Plata, Argentina*

[3]*Department of Physics, Emory University, Atlanta, GA 30322, USA*

(Dated: April 7, 2017)

Abstract

The relationship between anomalous superdiffusive behavior and particle trapping probability is analyzed on a rocking ratchet potential with spatially correlated weak disorder. The trapping probability allows us to obtain analytical expressions for the number of wells where a given number of particles get trapped. We have also calculated the second-moment of the particle distribution function C_2 as a function of time, when the untrapped particle has a constant velocity. We also use the expression for C_2 to characterize anomalous superdiffusive motion.

I. INTRODUCTION

Ratchets became a subject of interest more than five decades ago when Richard Feynman introduced them as an example of the impossibility of violating the second law of thermodynamics even in the presence of an asymmetric potential in a random environment [1]. Almost thirty years later they gained popularity in physics following Marcelo Magnasco's proposal that a net current may be obtained if a time-correlated force acts on the particle in an asymmetric potential [2]. The time correlation of the applied force is essential to get a net current without a net force on a Brownian particle moving in a ratchet potential. The asymmetric potential characteristic of ratchets often arises in systems where structural bottlenecks lead to quenched disorder [3]. Other examples include heterosubstrate-induced graphene superlattices in which zero-energy states emerge in the form of Dirac points in asymmetric potentials [4], and antisymmetric dc voltage drop along amorphous indium oxide wires exposed to an ac bias source [5].

When the thermal noise is negligible, the overdamped equation of motion accounts solely for effects of quenched disorder [6, 7] and may be used for the study of the dynamics of localized structures like domain walls, driven vortices in type-II superconductors and driven Wigner crystals [8–12]. The influence of uncorrelated quenched disorder, in the absence of thermal noise, on the diffusive motion of a periodically forced overdamped particle in ratchets was considered in previous works [13, 14]: Normal chaotic diffusive transport was found in [13] and a trapping mechanism is shown to appear in [14] whenever the quenched disorder strength is higher than a threshold value with coexistence of locked and running states producing anomalous superdiffusive behavior with several orders of magnitude growth of the diffusion coefficient. This pronounced enhancement over free thermal diffusion has been predicted theoretically [15] and observed experimentally [16] in weak disorder tilted potentials. Correlated spatial disorder exists in many disordered materials, such as polymers [17], porous materials [18], and glasses [19]. Long-range correlated spatial disorder has also been found to produce anomalous diffusion in an overdamped rocking ratchet without thermal noise [20].

Recently, particle diffusion in weak disordered tilted potentials was studied [21]. Besides diffusion enhancement [15, 16], other anomalous transport behavior such as subtransport, subdiffusion, and superdiffusion were found as a function of the driving force or the disorder correlation length [21].

In this work, we focus on the study of particle motion on a rocking ratchet potential with spatially correlated weak disorder [13, 14, 20]. Since the coexistence of locked and running states are responsible for the anomalous superdiffusive behavior, in this work we concentrate

on the particle trapping probability, namely the probability of existence of locked states, and its opposite behavior, the existence of running states.

The outline of this paper is as follows. In Sec. II we present the model and its associated dynamical equations. In Sec. III we numerically calculate the trapping probability and compare the result with an approximate exponential form. In Sec. IV we consider the same problem, but ask a different question, namely, what is the effect of disorder on the trapping probability? We also derive an analytical expression using the exponential form of the trapping probability. In Sec. V we characterize the anomalous diffusive motion using the second moment C_2 as a function of time when the velocity of non-trapped particle is constant. Finally, in Sec. VI we conclude with some comments and conclusions.

II. MODEL

We consider the overdamped motion of a particle in a ratchet potential $U(x)$ in the presence of quenched noise $\eta(x)$. The equation of motion is given by,

$$-\gamma\frac{dx}{dt} - \big(1-\sigma\big)\frac{dU}{dx} - \sigma\frac{d\eta}{dx} + A\sin(\omega t) = 0, \tag{1}$$

where γ is the friction coefficient, σ determines the relative strength of the ratchet potential and the quenched disorder, A is the amplitude and ω is the frequency of the sinusoidal driving force.

The deterministic ratchet-potential is represented by the sum of two sine functions with height V and wavelength λ as,

$$U(x) = -V\frac{\lambda}{2\pi}\left[\sin\Big(\frac{2\pi x}{\lambda}\Big) + \frac{1}{4}\sin\Big(\frac{4\pi x}{\lambda}\Big)\right]. \tag{2}$$

The spatial autocorrelation function of the ratchet potential has a maximum at:

$$G_U(0) = < U(x)U(x+0) > = \frac{1}{\lambda}\int_0^{\lambda} U^2(x)\,dx = 1.0625\frac{V^2}{2}\frac{\lambda^2}{(2\pi)^2}. \tag{3}$$

In order to make the strengths of the ratchet force and the quenched disorder comparable, we express the quenched disorder spatial autocorrelation in the form,

$$G_\eta(x) = 1.0625\frac{V^2}{2}\frac{\lambda^2}{(2\pi)^2}\ e^{-\dfrac{(2\pi)^2x^2}{2l^2}}, \tag{4}$$

where the length l is defined such that $\Lambda = l/\lambda$ is the width of the Gaussian distribution in dimensionless spatial dimension z, which we will define in the next paragraph.

Instead of using arbitrary values of model parameters, we normalize them by defining the dimensionless spatial variable z and the dimensionless temporal variables τ as: $z = 2\pi x/\lambda$

and $\tau = [(2\pi)^2 V/(\gamma\lambda^2)]t$. Using these parameters, the dimensionless form of the dynamical equation becomes,

$$-\frac{dz}{d\tau} - \big(1-\sigma\big)\frac{dU(z)}{dz} - \sigma\frac{d\eta(z)}{dz} + \Gamma sin(\Omega\tau) = 0, \tag{5}$$

where $\Gamma = A\lambda/(2\pi V)$ and $\Omega = \omega\gamma\lambda^2/[(2\pi)^2 V]$.

The force autocorrelation can be determined from the random potential autocorrelation:

$$G_F = -\frac{d^2 G_\eta}{dz^2} \tag{6}$$

Then,

$$G_F = 1.0625\frac{1}{2\Lambda^2}\left(1 - \frac{z^2}{\Lambda^2}\right)e^{-\frac{z^2}{2\Lambda^2}} \tag{7}$$

To solve Eq. 5, we first generates values of random force at positions $x = 0, x = \lambda, x = 2\lambda....$ We interpolate the values for other positions, as needed. To generate the random force values we use the method described in [22] with a finite-input-response filter (FIR filter) instead of an infinite-input-response filter (IIR filter) used in [22]. We used the FIR filter because we found FIR filters were always stable and could be generated faster. As a test, we found that the disorder autocorrelation obtained with this method obeys Eq. 7.

As seen from Eq. 7, for a given z, a decrease in Λ results in a decrease in the random-force potential autocorrelation. Thus, when the potential changes abruptly, its derivative, which is the random force, will develop high peaks that will trap the particles as they encounter regions of strong negative-force during their motion. We define a 'well' as the distance between two consecutive peaks of the ratchet potential. In dimensionless units, the range of z values for the nth well is $(n-1)2\pi < z < n2\pi$. As in previous work [13], we use the value Ω=0.1, and define v_ω as the speed of the particle per period defined as the number of wells the particle travels in a time period $T = 2\pi/\Omega$.

III. TRAPPING PROBABILITY DENSITY

We have carried out simulations with different realizations of the quenched disorder. Both the deterministic ratchet force and the external sinusoidal force are bounded, while the quenched disorder is not, because it has a Gaussian probability distribution. As a result, in an infinitely-long path any particle will get trapped sooner or later.

The simulation results for the spatial trapping probability $f_{tr}(z)$ as a function of distance z with $\Gamma = 1.475$, $\Lambda = 0.095$, and $\sigma = 0.025$ is shown in Fig. 1. The solid line is an exponential fit to the data. There is excellent agreement with the numerical data. We have found similar

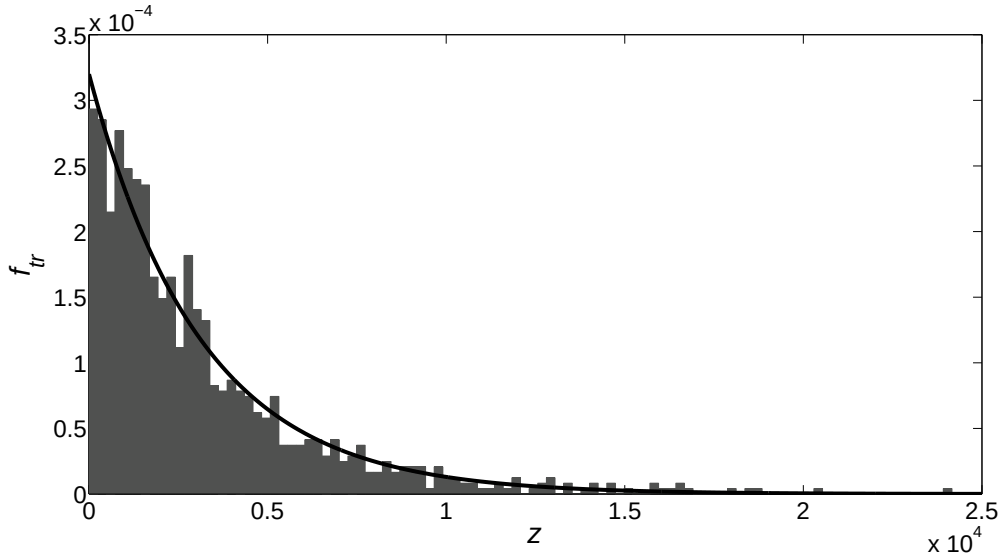

Figure 1. The spatial trapping probability $f_{tr}(z)$ is plotted as a function of distance z for 1,000 particles released at $z = 0$. The solid line is an exponential fit to the data using Eq. 8.

quality fits to the data for other values of Γ and Λ. As a consequence, the spatial trapping probability density may be approximated by the exponential function of the form,

$$f_{tr}(z) = \alpha_P e^{-\alpha_P z}, \tag{8}$$

where α_P is the value of the exponential function at $z = 0$. Figure 2 is a semi-log graph of

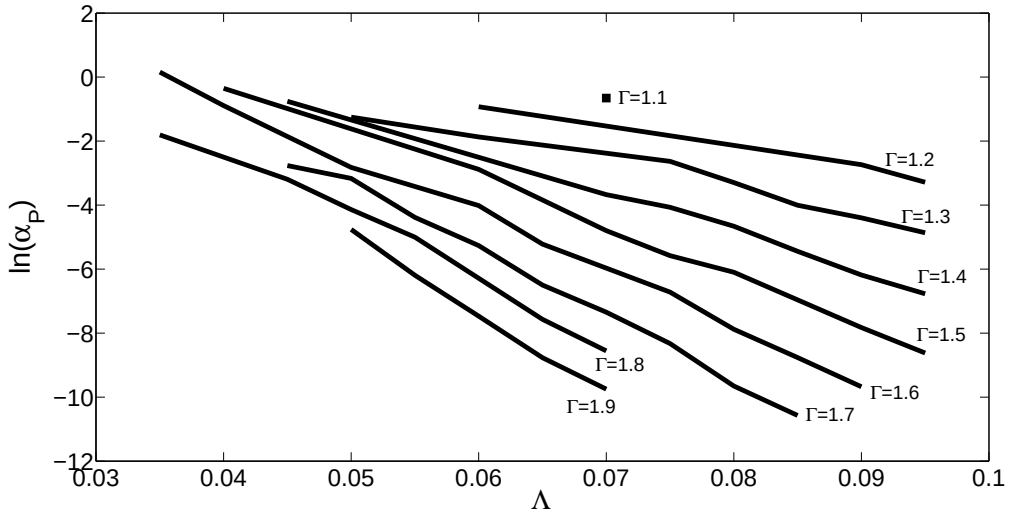

Figure 2. Semi-log plot of α_P as a function of the disorder correlation length Λ, for different values of Γ and $\sigma = 0.025$, indicates that α_P decays exponentially with Λ.

α_P as a function of Λ for different values of Γ for $\sigma = 0.025$. The results show that α_P has an approximately exponential decay with Λ. The reason the lines have different lengths is that we have only taken into account values of Λ and Γ for which the spatial trapping probability

density intercept was within 20% of the value of α_P in the exponent. This does not mean that the exponent is not always the additive inverse of the intercept. The problem is that for large Γ and Λ there are not sufficient number of trapped particles to obtain good statistics. On the other hand, when Γ and Λ are small, most particles get trapped close to the starting position causing poor statistics as well. As expected, when Γ increases, the number of trapped particles decreases, and therefore α_P also decreases. In addition, when Λ decreases, the RMS value of the quenched-disorder force increases (See Eq. 7), causing an increase in the probability of getting trapped leading to an increase in the value of α_P. This is consistent with Fig. 2.

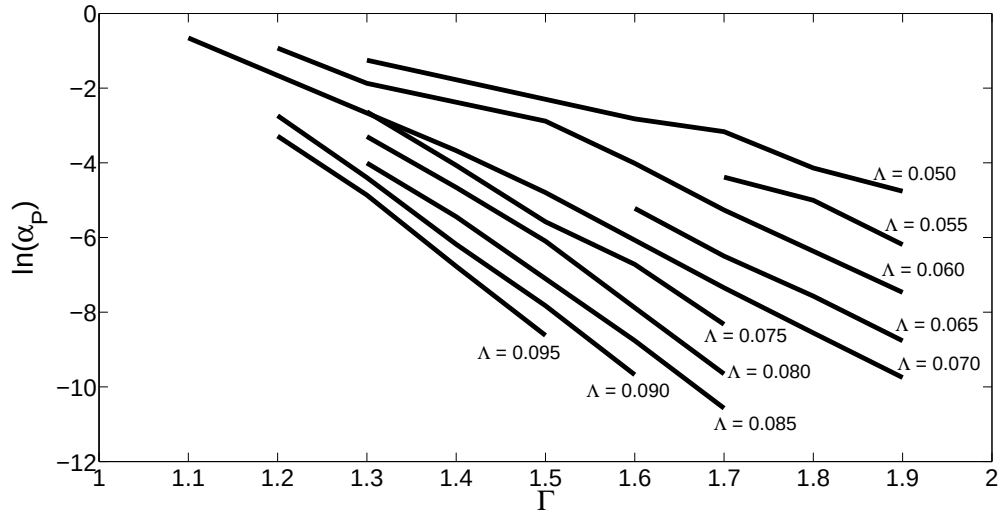

Figure 3. Semi-log plot of α_P as a function of the applied force amplitude Γ for different values of Λ has an approximately linear behavior.

In Fig. 3 we plot $\ln(\alpha_P)$ as a function of Γ for different values of Λ. The dependence of $\ln(\alpha_P)$ on Γ appears to be approximately linear. We expect that the trapping probability density function as a function of time has a similar form as Eq. 8 and can be written as,

$$f_{tr}(\tau) = \alpha_T e^{-\alpha_T \tau} \tag{9}$$

In order to test whether α_T decays exponentially with Γ and Λ we plot both α_P and α_T on a semi-log plot as a function of Λ in Fig. 4. The slopes of the two curves are not the same. Notice that when Λ=0.055, $\ln(\alpha_P) - \ln(\alpha_T)$=10 and when Λ=0.1, $\ln(\alpha_P) - \ln(\alpha_T)$=5. Taking into account that the time period equals ten times the spatial period in this case, we arrive at the conclusion that the gradually-changing value of the average speed from $< v >= v_\omega$ to $< v >= 2v_\omega$ as Λ goes from 0.055 to 0.1 is the reason for the change in the slope of the α_T curve.

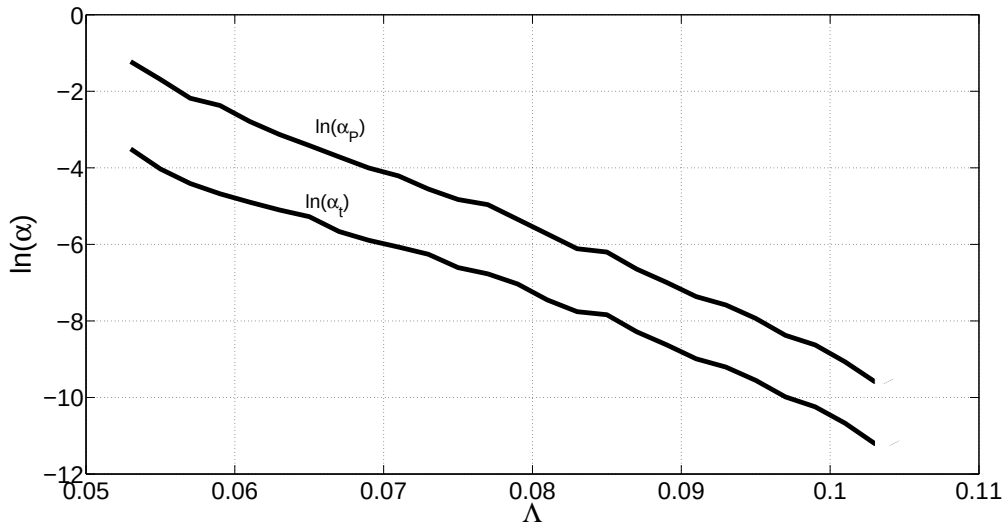

Figure 4. Semi-log plots of α_P and α_T as a function of Λ, for $\Gamma = 1.47$. Notice that $(\alpha_P/\alpha_T) = 10$ for $\Lambda = 0.053$ while $(\alpha_P/\alpha_T) = 5$ for $\Lambda = 0.103$. This is because of the change in the particle mean velocity. This causes the slopes of the two curves to be different.

IV. NUMBER OF WELLS WHERE A GIVEN NUMBER OF PARTICLES ARE TRAPPED

We may wonder: if we let N particles travel, each of them with a different disorder realization, what is the most-likely number of wells in which M particles will get trapped? In order to answer this question we use Eq. 8 to calculate the cumulative distribution function,

$$F_{tr}(z) = 1 - e^{-\alpha_P z}. \tag{10}$$

Using Eq. 10 we can calculate the probability that a particle gets trapped at well n as:

$$P_n = e^{-\alpha_P (n-1)2\pi} - e^{-\alpha_P n 2\pi}. \tag{11}$$

As a result, the probability that a particle that started moving at z=0 arrives at well n is given by,

$$1 - F_{tr}((n-1)2\pi) = e^{-\alpha_P (n-1)2\pi}. \tag{12}$$

Therefore, the probability p_n of getting trapped at *well* n for an arriving particle is the ratio of the probability of getting trapped at well n divided by the probability of arriving at well n:

$$p_n = \frac{P_n}{1 - F_{tr}(2(n-1)\pi)} = 1 - e^{-\alpha_P 2\pi}. \tag{13}$$

Finally, the probability for an arriving particle to get trapped at *any well* is,

$$p_n = p = 1 - e^{-\alpha_P 2\pi}. \tag{14}$$

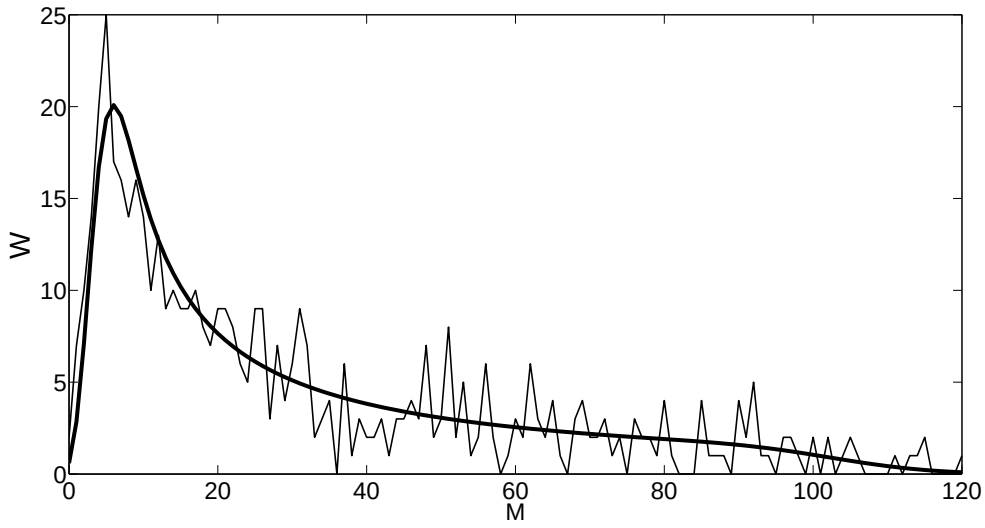

Figure 5. The prediction of Eq. 17 for the average number of wells $\overline{W(M)}$ where M particles get trapped is shown as solid line. For comparison we have also plotted the simulation results for $N = 16,000$ particles, with $Q = 500$ wells from $z = 0$ to $z = 500$ with $\Gamma = 1.5$, $\Lambda = 0.085$, and $\sigma = 0.025$ for which $\alpha_P = 0.00104$.

If a large amount N of particles evolve from $z = 0$, the number of particles arriving at well n will be $K(n) = [N \exp(-\alpha_P(n-1)2\pi)]$, and the chance that M particles will get trapped at well n is equal to,

$$P_M(n) = \begin{pmatrix} K(n) \\ M \end{pmatrix} p^M (1-p)^{K(n)-M}. \tag{15}$$

When $K(n) >> M$, we can approximate the Binomial distribution with the Poisson distribution:

$$P_M(n) \approx \frac{e^{-K(n)p} \{K(n)p\}^M}{M!} \tag{16}$$

If we consider the first Q wells, the average number of wells where M particles are trapped is obtained as the sum of the probabilities $P_M(n)$ of getting trapped in each well, since independence of these events is assumed, namely:

$$\overline{W(M)} \approx \sum_{n=1}^{Q} \frac{e^{-K(n)p} \{K(n)p\}^M}{M!} \tag{17}$$

Eq. 17 is plotted as a solid line in Figs. 5 and 6 long with the simulation results for N=16,000 particles. In Figs. 5 and 6 values of Q are 500 and 1,000, respectively.

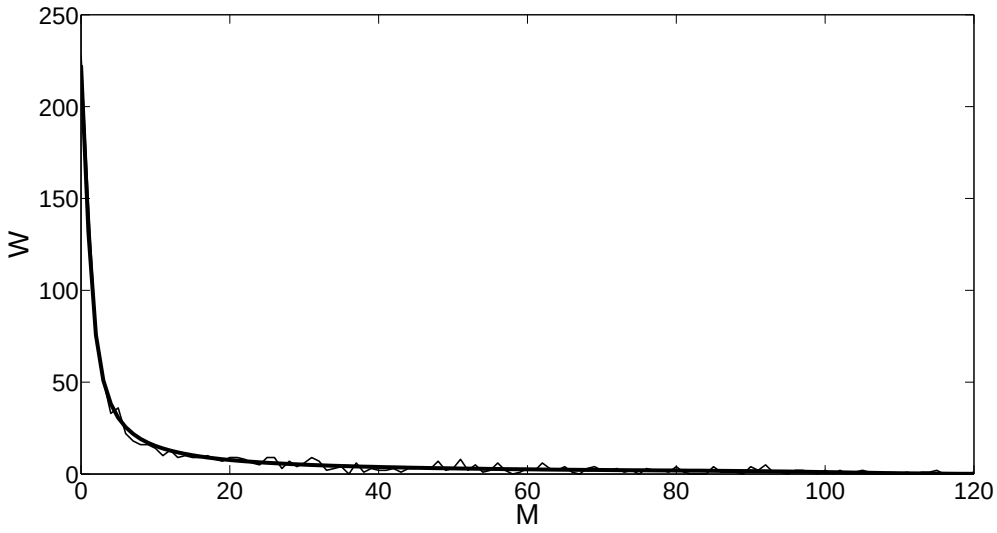

Figure 6. The same conditions as Fig. 5 but now with $Q = 1,000$. As new far-away-from-the-origin wells are considered, more cases of wells with few trapped particles appear. The solid line is the prediction of Eq. 17 and gives and excellent fit to the simulation data.

V. CHARACTERIZATION OF ANOMALOUS DIFFUSION

To characterize the nature of the anomalous diffusion we now concentrate on the second moment $C_2(\tau) = \overline{z(\tau)^2} - \overline{z(\tau)}^2$. Let us assume that all particles were released at τ=0, and $z = 0$, but they experienced different realizations of quenched disorder. After time τ the particle has moved across s wells and the particle density is given by,

$$f(z) = \alpha_P e^{-\alpha_P z}\big[u(z) - u(z - sv_\omega\tau)\big] + \delta\big(z - sv_\omega\tau\big)\int_{sv_\omega\tau}^{\infty} \alpha_P e^{-\alpha_P z} dz, \tag{18}$$

where $u(z)$ is the Heaviside step function. Eq. 18 can be explained by assuming that particles that have not been trapped by time τ are all located at $z = sv_\omega\tau$. This is because the particles that have not been trapped have a single velocity value. The average position can be calculated from Eq. 18:

$$\overline{z(\tau)} = \int_0^{sv_\omega\tau} z\alpha_P e^{-\alpha_P z} dz + (sv_\omega\tau)\int_{sv_\omega\tau}^{\infty} \alpha_P e^{-\alpha_P z} dz = \frac{1 - e^{-\alpha_T\tau}}{\alpha_P}, \tag{19}$$

where we have used the fact that $\alpha_P s v_\omega \tau = \alpha_T$. The mean of z squared is then given by,

$$\overline{z(\tau)^2} = \int_0^{sv_\omega\tau} z^2\alpha_P e^{-\alpha_P z} dz + (sv_\omega\tau)^2\int_{sv_\omega\tau}^{\infty} \alpha_P e^{-\alpha_P z} dz. \tag{20}$$

Combining these results, we can calculate the second cumulant,

$$C_2 = \overline{z(\tau)^2} - \overline{z(\tau)}^2 = \frac{[1 - 2\alpha_T\tau e^{-\alpha_T\tau} - e^{-2\alpha_T\tau}]s^2 v_\omega^2}{\alpha_T^2}. \tag{21}$$

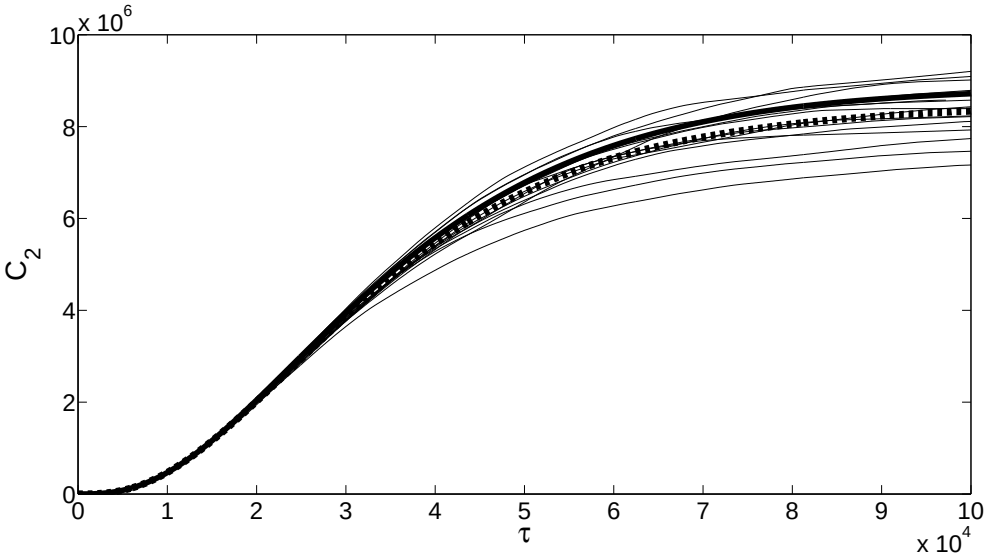

Figure 7. Second moment as a function of the normalized time. In this case $\Gamma = 1.47$, $\lambda = 0.095$. Each thin line was built by solving the differential equation for 1,000 particles, each of them experiencing a different realization of disorder. The thick dotted line is the average of the simulation data. The thick solid line is the prediction of Eq. 21, with $\alpha_P = 0.000337$, $\alpha_T = 0.0000672$ and $s = 2$.

In order to test Eq. 21, we numerically solved Eq. 5 for 1,000 particles that were allowed to evolve from z=0 for a time τ. The thick solid line in Fig. 7 is from Eq. 21 and the thin lines are the results of numerical simulations. Eq. 21 gives a good fit to the data in the interval before the saturation regime. In order to explore this region in more detail, in Fig. 8 we show a log-log plot of C_2 as a function of τ. The solid line is the result of the simulations with 1,000 particles and the dashed line is the result of Eq. 21. For an extended range of values of τ the results indicate that C_2 grows with a power law of the form,

$$C_2 = A\tau^{\beta}. \tag{22}$$

In early times, particles are not yet trapped and the motion is ballistic with an exponent $\beta \approx 2$. In the intermediate times there are both trapped and running particles and over an extended time period, from $\tau \approx 10^2$ to 10^4, the motion is superdiffusive with an exponent $\beta \simeq 2.8$. Beyond $\tau > 10^4$, C_2 slowly levels off and crosses over to the saturation region, where particles are trapped. Our analytic result, Eq. 21, is in excellent agreement with the data in the intermediate region, because we assume a continuous process that is only valid at longer time, before saturation.

We have obtained another estimate for β from the expression for C_2, Eq. 21, at $\tau_1 = 1/(8\alpha_T)$ and $\tau_2 = 1/(4\alpha_T)$. For $\tau = \tau_1$ it is expected that 11.78% of particles are trapped. For $\tau = \tau_2$ it is expected that 22.12% of particles are trapped. Those τ values were chosen so that C_2 had

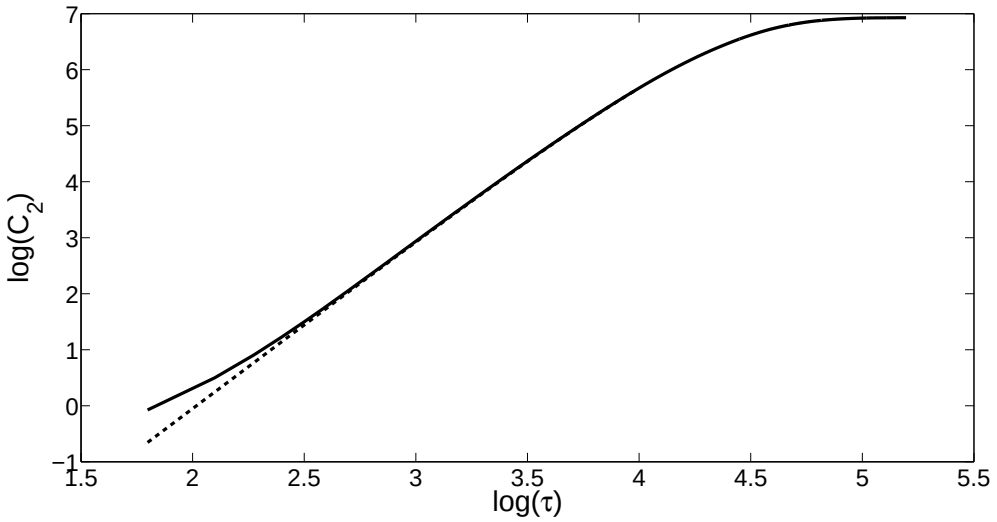

Figure 8. Log-log plot of C_2 versus τ. The solid line is from simulations with 1,000 particles. The dotted line is the prediction of Eq. 21. In early times the particle motion is ballistic, but over an extended range of time, both our analytic result and the simulations show that the motion is superdiffusive with an exponent $\beta \simeq 2.8$

not yet reached the saturation regime. From these considerations we can find β,

$$C_2(\tau_1) = A\ \tau_1^{\beta} = 0.004069\ \frac{v_\omega^2\ v_r^2}{\alpha_T^2} \tag{23}$$

$$C_2(\tau_2) = A\ \tau_2^{\beta} = 0.000575\ \frac{v_\omega^2\ v_r^2}{\alpha_T^2} \tag{24}$$

$$\beta = \log_2\left[\frac{C_2(\tau_2)}{C_2(\tau_1)}\right] = 2.82 \tag{25}$$

This result agrees well with the slope of the log-log plot in Fig. 8. Common logarithm is used. We note that the value of β does not depend on α_T or s, provided there is just one velocity value for those particles that have not still been trapped. From Eq. 21 we see that there are two exceptions: $\alpha_T = 0$ and $\alpha_T \to \infty$. In both cases $C_2 = 0$. When $\alpha_T = 0$ there is no disorder at all. Then all particles move at the same velocity. When $\alpha_T \to \infty$ all particles get trapped in the first well.

VI. CONCLUSIONS

In this paper, we have studied the role of correlated weak quenched disorder on superdiffusive transport in a ratchet potential. The particles all experience different realizations of quenched disorder. We have shown that the influence of correlated quenched disorder allows the presence of both running and trapped particles.

In order to elucidate the relationship between anomalous superdiffusion and particle trapping we focused on the particle trapping probability density function. We showed that a decreasing exponential function, with exponents α_P and α_T that characterize the space and time dependence of the density function, respectively, provides an excellent fit to the trapping probability density function. We also show that an exponential form gives excellent fit to our data for the dependence of α_P on both the disorder correlation length Λ and the applied force amplitude Γ. However, α_T does not show an exponential behavior, because it depends on the average particle velocity as well. Based on these results, we derive an analytical expression for the average number of wells where a given number of particles get trapped.

Finally, in an attempt to characterize superdiffusive motion, we obtain an analytic expression for the second-moment distribution function C_2 as a function of time, when the particle velocity of particles that are not trapped is assumed to be constant. Assuming that C_2 has a power law behavior with exponent β, we find a good fit to both our analytic expression for C_2 and the simulation results with $\beta = 2.82$, indicating anomalous superdiffusive motion.

---

[1] J. Zheng, X. Zheng, C. Yam, and G. Chen, Phys. Rev. E **81**, 061104 (2010).

[2] M. Magnasco, Physical Review Letters **71**, 1477 (1993).

[3] T. Chou and G. Lakatos, Physical Review Letters **93**, 198101 (2004).

[4] X. Fan, W. Huang, T. Ma, and L. G. Wang, Physical Review B **93**, 165137 (2016).

[5] P. S., E. Shimsoni, and A. Frydman, Physical Review B **84**, 014529 (2011).

[6] S. I. Denisov, M. Kostur, E. S. Denisova, and P. Hänggi, Phys. Rev. E **76**, 031101 (2007).

[7] S. I. Denisov, T. Lyutyy, E. S. Denisova, P. Hänggi, and H. Kantz, Phys. Rev. E **79**, 051102 (2009).

[8] C. J. Olson, C. Reichhardt, and F. Nori, Physical Review B **81**, 3757 (1998).

[9] F. Pardo, de la Cruz F., G. P., B. E., and D. J. Bishop, Nature(London) **396**, 348 (1998).

[10] M. C. Hellerquist, D. Ephron, W. R. White, M. R. Beasley, and A. Kapitulnik, Physical Review Letters **76**, 4022 (1996).

[11] A. M. Troyanovski, J. Aarts, and K. P. H., Nature(London) **399**, 665 (1999).

[12] C. Reichhardt, C. J. Olson, N. J. Gronbech-Jensen, and F. Nori, Physical Review Letters **86**, 4354 (2001).

[13] M. N. Popescu, C. M. Arizmendi, A. L. Salas-Brito, and F. Family, Physical Review Letters **85**, 3321 (2000).

[14] D. G. Zarlenga, H. A. Larrondo, C. M. Arizmendi, and F. Family, Phys. Rev. E **75**, 051101

(2007).

[15] P. Reimann and R. Eichhorn, Physical Review Letters **101**, 180601 (2008).

[16] S.-H. Lee and D. G. Grier, Physical Review Letters **96**, 190601 (2006).

[17] A. Cioroianu, E. Spiesz, and C. Storm, Journal of the Mechanics and Physics of Solids **89**, 110 (2016).

[18] P. M. Adler, *Porous Media: Geometry and Transport* (Reed Publishing (USA) Inc., 230 Park Avenue, 7th floor, New York, NY 10169, USA, 1992).

[19] L. Berthier and G. Bertoli, Reviews of Modern Physics **83**, 587 (2011).

[20] L. Gao, X. Luo, S. Zhu, and B. Hu, Phys. Rev. E **67**, 062104 (2003).

[21] M. Khoury, A. M. Lacasta, J. M. Sancho, and K. Lindenberg, Phys. Rev. Lett. **106**, 090602 (2011).

[22] A. Rodriguez and S. Johnson, arXiv:physics , 0703152v4 (2007).